

# A new stability analysis of variable time step central difference method for transient dynamics viscoelastic problems

Benjamin Georgette<sup>✉</sup> · David Dureisseix<sup>✉</sup> · Anthony Gravouil<sup>✉</sup>

Received: date / Accepted: date

**Abstract** In this paper, we propose a general framework for studying the stability properties of the central difference scheme for transient dynamics viscoelastic problems using both constant and variable time step. First, we introduce a new explicit constant time step integration method for viscoelastic materials. This new method surpasses the stability limits of Belytschko's half-lagged velocity approximation. Second, we provide a new stability analysis of the variable time step central difference method. The proposed analysis shows that central difference's stability can be ensured only thanks to the zero-stability criteria, based on the multistep formulation of the method. Without viscous damping, ensuring stability requires to decrease, or at least to maintain constant time step during the time integration. However, with viscous damping, there is a slight possibility of increasing the time step during the time integration process.

**Keywords** Central difference method · Stability analysis · Variable time step · Viscoelasticity · Transient dynamics

**Mathematics Subject Classification (2020)** 65L06 · 65L20 · 74D05 · 74S99

## 1 Introduction

Explicit integration schemes are attractive for solving transient dynamics problems due to their potential computing speed, enabled by the possibility of matrix-free resolution [14, 5, 4]. The properties of such integration schemes have been studied over the past decades. According to Lax's equivalence theorem [18], accuracy and stability are necessary and sufficient for convergence. This paper focuses on the central difference method, also known as the Leapfrog, the Stormer-Verlet, or the Newmark method with parameters  $\gamma = 1/2, \beta = 0$  [21, 9, 2, 10]. Its structure preserving, symplectic property [23, 7] further motivates our study.

Biomechanics use explicit time integration for soft tissues for the many, already cited, advantages of such methods [22, 20, 15]. In particular, explicit integration of transient viscoelastic problems is challenging. Indeed, the integration of the viscous stress-strain relationship for a classic Kelvin material results in implicit scheme. Belytschko proposed one approximation method [2] to address this issue. In this paper, we introduce a new explicit constant time step integration method for continuum viscoelastic material, called the  $\alpha$  viscous stress averaging scheme. We show that our method generalises Belytschko's approximation, and has better stability properties.

Variable time step schemes have stability properties that must be analysed carefully. The symplectic property of the central difference scheme has been shown to be strongly impacted by changes in the time step during integration [26, 3]. Furthermore, previous studies of the stability of the variable time-step central difference scheme have demonstrated that one choice of a time step affects the following time step; a time grid constructed without careful consideration might easily lead to an unstable integration and unreliable results [24, 25, 27]. Therefore, bounds for the evolution of the time step have been calculated [27] by conducting a spectral stability analysis of the one-step formulation of the central difference method (a classical analysis for constant time steps [9]). However, we prove in this paper that only the zero-stability analysis [6], based on the formulation of the central difference method as a linear multistep method, leads to a relevant analysis.

The present paper is organized as follows. After introducing the standard semi-discrete equation of motion for structural dynamics (section 2), section 3 presents the new  $\alpha$  viscous stress averaging scheme for transient viscoelastic problems. Then, section 4 provides the main results of the paper concerning the behaviour of the

variable time step central difference time integrator.

*Notations*

*Roman face, greek face*  $\rho, S, E$ : Scalars.

*Lower case italic bold face*  $\mathbf{u}, \mathbf{v}$ : Vectors and vector fields.

*Upper case italic bold face*  $\mathbf{U}$ : Nodal finite element vectors.

*Upper case greek face*  $\Omega, \Gamma$ : Sets representing bodies and frontiers.

*Lower case greek bold face*  $\boldsymbol{\sigma}, \boldsymbol{\varepsilon}$ : Tensors of order 2.

*Upper case bold face*  $\mathbf{A}, \mathbf{M}$ : Matrices.

*Upper case script*  $\mathcal{U}, \mathcal{T}$ : Sets.

*Upper case calligraphic*  $\mathcal{L}, \mathcal{S}$ : Functions and functionnals.

*Upper case blackboard bold*  $\mathbb{H}, \mathbb{I}$ : Tensors of order 4.

## 2 The semi-discrete equations of structural dynamics

Let us consider  $\Omega$  a continuous body of density  $\rho$ , with  $\Gamma$  its boundary, of outward normal  $\mathbf{n}$ . The boundary  $\Gamma$  is divided into two distinct parts,  $\Gamma_D$  is submitted to Dirichlet's boundary conditions, i.e. displacement imposed boundary,  $\Gamma_N$  is submitted to Neumann, i.e. strength imposed boundary, such that  $\Gamma = \Gamma_D \cup \Gamma_N$  and  $\Gamma_D \cap \Gamma_N = \emptyset$ . Bulk forces  $\mathbf{f}_d$  are imposed to the body. We assume that perturbations are sufficiently small to use the linearized Cauchy-Green tensor  $\boldsymbol{\varepsilon}(\mathbf{u})$ .  $\mathbf{x} \in \Omega$  denotes a position on the body, while  $\mathbf{u}$  and  $\mathbf{v}$  denote displacement and velocity, respectively, of a point in the body. The Cauchy stress tensor  $\boldsymbol{\sigma}$  is related to strain through the stress-strain law  $\boldsymbol{\sigma} = f(\boldsymbol{\varepsilon}, \dot{\boldsymbol{\varepsilon}})$ . During the time interval  $\mathcal{T} = [t_0, t_f]$ , the strong form of the problem  $\forall t \in \mathcal{T}$  is given by

$$\operatorname{div}(\boldsymbol{\sigma}) + \mathbf{f}_d = \frac{\partial \mathbf{p}}{\partial t} \quad \forall \mathbf{x} \in \Omega \quad (1)$$

$$\boldsymbol{\sigma} \cdot \mathbf{n} = \mathbf{t}_d \quad \forall \mathbf{x} \in \Gamma_N \quad (2)$$

$$\boldsymbol{\varepsilon} = \frac{1}{2} \left( \frac{\partial \mathbf{u}}{\partial \mathbf{x}} + \frac{\partial \mathbf{u}^\top}{\partial \mathbf{x}} \right) \quad \forall \mathbf{x} \in \Omega \quad (3)$$

$$\mathbf{v} = \frac{\partial \mathbf{u}}{\partial t} \quad \forall \mathbf{x} \in \Omega \quad (4)$$

$$\mathbf{u} = \mathbf{u}_d \quad \forall \mathbf{x} \in \Gamma_D \quad (5)$$

$$\boldsymbol{\sigma} = f(\boldsymbol{\varepsilon}, \dot{\boldsymbol{\varepsilon}}) \quad \forall \mathbf{x} \in \Omega \quad (6)$$

$$\mathbf{p} = \rho \mathbf{v} \quad \forall \mathbf{x} \in \Omega \quad (7)$$

We introduce the set of virtual displacement

$$\mathcal{U}_0^{[\mathbf{x}]} := \{ \mathbf{u} \in \mathcal{H}^1(\Omega) | \mathbf{u}(\mathbf{x}) = \mathbf{0} \quad \forall \mathbf{x} \in \Gamma_D \} \quad (8)$$

with  $\mathcal{H}^1$  the standard Hilbert space. The spatial weak form of the problem is obtained thanks to the previous strong form

$$\begin{aligned} \forall \mathbf{u}^* \in \mathcal{U}_0^{[\mathbf{x}]}, \forall t \in \mathcal{T}, \\ - \int_{\Omega} \boldsymbol{\sigma} : \boldsymbol{\varepsilon}(\mathbf{u}^*) d\Omega + \int_{\Gamma_N} \mathbf{t}_d \cdot \mathbf{u}^* d\Gamma + \int_{\Omega} \mathbf{f}_d \cdot \mathbf{u}^* d\Omega - \int_{\Omega} \rho \frac{\partial \mathbf{v}}{\partial t} \cdot \mathbf{u}^* d\Omega = 0 \end{aligned} \quad (9)$$

Next developments consider a Kelvin viscoelastic material, for which viscous strains can be split into an elastic part  $\boldsymbol{\sigma}^e = \mathbb{H} : \boldsymbol{\varepsilon}(\mathbf{u})$ , with  $\mathbb{H}$  the Hooke's fourth order elasticity tensor, and a viscous part  $\boldsymbol{\sigma}^v$  as:

$$\boldsymbol{\sigma} = \boldsymbol{\sigma}^e + \boldsymbol{\sigma}^v \quad (10)$$

We consider a finite element approximation on displacements

$$\mathbf{u}(\mathbf{x}, t) = \sum_{i=0}^{N_{\text{nodes}}} \mathbf{s}^i(\mathbf{x}) u^i(t) \quad (11)$$

where  $\mathbf{s}$  are shape functions, and  $\cdot^i$  denotes the node's number. We obtain the following form of the problem

$$\sum_{i=0}^{N_{\text{nodes}}} (u^*)^i(t) \cdot \left\{ - \sum_{j=0}^{N_{\text{nodes}}} \left( \int_{\Omega} (\mathbb{H} : \boldsymbol{\varepsilon}(\mathbf{s}^i(\mathbf{x})) : \boldsymbol{\varepsilon}(\mathbf{s}^j(\mathbf{x}))) d\Omega u^j(t) \right) + \right. \\ - \int_{\Omega} \boldsymbol{\sigma}^v : \boldsymbol{\varepsilon}(\mathbf{s}^i(\mathbf{x})) d\Omega + \\ + \int_{\Gamma_N} \mathbf{t}_d \cdot \mathbf{s}^i(\mathbf{x}) d\Gamma + \int_{\Omega} \mathbf{f}_d \cdot \mathbf{s}^i(\mathbf{x}) d\Omega + \\ \left. - \sum_{j=0}^{N_{\text{nodes}}} \left( \int_{\Omega} (\mathbf{s}^i(\mathbf{x}) \cdot \rho \cdot \mathbf{s}^j(\mathbf{x})) d\Omega \frac{dv^j(t)}{dt} \right) \right\} = 0 \quad (12)$$

One can identify the components of the mass matrix  $M^{ij} = \int_{\Omega} \mathbf{s}^i(\mathbf{x}) \cdot \rho \cdot \mathbf{s}^j(\mathbf{x}) d\Omega$ , symmetric positive definite, the components of the stiffness matrix  $K^{ij} = \int_{\Omega} \mathbb{H} : \boldsymbol{\varepsilon}(\mathbf{s}^i(\mathbf{x})) : \boldsymbol{\varepsilon}(\mathbf{s}^j(\mathbf{x})) d\Omega$ , and the components of the nodal viscous force  $(F^v(\sigma^v)(t))^i = \int_{\Omega} \boldsymbol{\sigma}^v : \boldsymbol{\varepsilon}(\mathbf{s}^i(\mathbf{x})) d\Omega$ . This equation holds true for all virtual displacement  $(u^*)^i$ , such that the former equation leads to the semi discretized equation of transient dynamics, with  $\mathbf{U}$  and  $\mathbf{V}$  denoting respectively the finite element nodal displacement and velocity:

$$\mathbf{V}(t) = \frac{d\mathbf{U}}{dt}(t) \quad (13)$$

$$\mathbf{M} \frac{d\mathbf{V}}{dt}(t) = \mathbf{F}^{\text{ext}}(t) - \mathbf{F}^{\text{int}}(t) \quad (14)$$

$$\mathbf{F}^{\text{ext}}(t) = \left( \dots (F^{\text{ext}}(t))^i \dots \right)^T \quad (15)$$

$$\text{with } (F^{\text{ext}}(t))^i = \int_{\Gamma_N} \mathbf{t}_d(\mathbf{x}, t) \cdot \mathbf{s}^i(\mathbf{x}) d\Gamma + \int_{\Omega} \mathbf{f}_d(\mathbf{x}, t) \cdot \mathbf{s}^i(\mathbf{x}) d\Omega \quad (16)$$

$$\mathbf{F}^{\text{int}}(t) = \left( \dots (F^{\text{int}}(t))^i \dots \right)^T \quad (17)$$

$$\text{with } (F^{\text{int}}(t))^i = \Sigma_{j=0}^{N_{\text{nodes}}} K^{ij} u^j(t) + \int_{\Omega} \boldsymbol{\sigma}^v : \boldsymbol{\varepsilon}(\mathbf{s}^i(\mathbf{x})) d\Omega \quad (18)$$

Equation (14) is a second order ordinary differential equation in time, integrated with the central difference method. The dependence of internal forces on displacement and velocity determines the specific problem to be solved, directly impacting the properties of the integration scheme.

### 3 Constant time step

#### 3.1 The central difference scheme for transient dynamics

In this section, we develop the formulation of the central difference scheme thanks to the discrete Euler-Lagrange equations. We consider the semi-discretized Lagrangian associated to the problem depicted in the last section:

$$\mathcal{L}(\mathbf{U}, \mathbf{V}) = \mathcal{T}(\mathbf{V}) - \mathcal{P}(\mathbf{U}) = \frac{1}{2} \mathbf{V}^T \mathbf{M} \mathbf{V} - \mathcal{P}(\mathbf{U}) \quad (19)$$

with  $\mathbf{M}$  the mass matrix, symmetric positive definite, and  $\mathcal{P}$  the potential function associated to the nodal internal and external forces, with  $\nabla \mathcal{P}(\mathbf{U}) = \mathbf{F}^{\text{ext}} - \mathbf{F}^{\text{int}}$ . The action integral:

$$\mathcal{S}[\mathbf{U}] = \int_{\mathcal{T}} \mathcal{L}(\mathbf{U}, \mathbf{V}) dt \quad (20)$$

satisfies the Hamilton's principle [1]:

$$\delta \mathcal{S}[\mathbf{U}] = 0 \quad \forall \delta \mathbf{U}, \delta \mathbf{U}(t_0) = \delta \mathbf{U}(t_f) = 0 \quad (21)$$

We consider the time interval  $\mathcal{T}$ , split with a uniform time step grid, with  $N_t$  time steps, and  $\Delta t$  the length of the time step, such that  $\Delta t = (t_f - t_0)/N_t$ . Quantities at time  $t_n = t_0 + n\Delta t$  are now denoted  $\cdot_n$ . Let  $\mathcal{S}_d$  be the discrete action associated to the Lagrangian  $\mathcal{L}$  as:

$$\mathcal{S}_d = \sum_{n=0}^{N_t-1} \int_{t_n}^{t_n + \Delta t} \mathcal{L}(\mathbf{U}(t), \mathbf{V}(t)) dt = \sum_{n=0}^{N_t-1} \mathcal{L}_d(\mathbf{U}_n, \mathbf{U}_{n+1}, \Delta t) \quad (22)$$

where  $\mathcal{L}_d$  is the discrete Lagrangian, approximated with the rectangle rule [16, 19]:

$$\mathcal{L}_d(\mathbf{U}_n, \mathbf{U}_{n+1}, \Delta t) = \Delta t \left[ \frac{1}{2} \left( \frac{\mathbf{U}_{n+1} - \mathbf{U}_n}{\Delta t} \right)^T \mathbf{M} \left( \frac{\mathbf{U}_{n+1} - \mathbf{U}_n}{\Delta t} \right) - \mathcal{P}(\mathbf{U}_n) \right] \quad (23)$$

Then, the discrete Hamilton's principle holds:

$$\begin{aligned} \forall \delta \mathbf{U}_n | \delta \mathbf{U}_0 = \delta \mathbf{U}_{N_t} = \mathbf{0}, \\ \delta \mathcal{S}_d = 0 \Leftrightarrow \sum_{n=0}^{N_t-1} (\mathbf{D}_1 \mathcal{L}_d(\mathbf{U}_n, \mathbf{U}_{n+1}, \Delta t) \delta \mathbf{U}_n + \mathbf{D}_2 \mathcal{L}_d(\mathbf{U}_n, \mathbf{U}_{n+1}, \Delta t) \delta \mathbf{U}_{n+1}) = 0 \\ \Leftrightarrow \sum_{n=1}^{N_t-1} (\mathbf{D}_1 \mathcal{L}_d(\mathbf{U}_n, \mathbf{U}_{n+1}, \Delta t) + \mathbf{D}_2 \mathcal{L}_d(\mathbf{U}_{n-1}, \mathbf{U}_n, \Delta t)) \delta \mathbf{U}_n + \\ + \mathbf{D}_1 \mathcal{L}_d(\mathbf{U}_0, \mathbf{U}_1, \Delta t) \delta \mathbf{U}_0 + \mathbf{D}_2 \mathcal{L}_d(\mathbf{U}_{N_t-1}, \mathbf{U}_{N_t}, \Delta t) \delta \mathbf{U}_{N_t} = 0 \\ \Leftrightarrow \sum_{n=0}^{N_t-2} (\mathbf{D}_1 \mathcal{L}_d(\mathbf{U}_{n+1}, \mathbf{U}_{n+2}, \Delta t) + \mathbf{D}_2 \mathcal{L}_d(\mathbf{U}_n, \mathbf{U}_{n+1}, \Delta t)) \delta \mathbf{U}_{n+1} + \\ + \mathbf{D}_1 \mathcal{L}_d(\mathbf{U}_0, \mathbf{U}_1, \Delta t) \delta \mathbf{U}_0 + \mathbf{D}_2 \mathcal{L}_d(\mathbf{U}_{N_t-1}, \mathbf{U}_{N_t}, \Delta t) \delta \mathbf{U}_{N_t} = 0 \end{aligned} \quad (24)$$

Since  $\delta \mathbf{U}_0 = \delta \mathbf{U}_{N_t} = \mathbf{0}$ , we obtain the discrete Euler-Lagrange equations:

$$\mathbf{D}_1 \mathcal{L}_d(\mathbf{U}_{n+1}, \mathbf{U}_{n+2}, \Delta t) + \mathbf{D}_2 \mathcal{L}_d(\mathbf{U}_n, \mathbf{U}_{n+1}, \Delta t) = 0 \quad (25)$$

with the partial derivatives ( $\mathbf{D}_1$  and  $\mathbf{D}_2$ ) defined as

$$\mathbf{D}_1 \mathcal{L}_d(\mathbf{U}_{n+1}, \mathbf{U}_{n+2}, \Delta t) = - \left[ \frac{1}{\Delta t} \mathbf{M}(\mathbf{U}_{n+2} - \mathbf{U}_{n+1}) + \Delta t \nabla \mathcal{P}(\mathbf{U}_{n+1}) \right] \quad (26)$$

$$\mathbf{D}_2 \mathcal{L}_d(\mathbf{U}_n, \mathbf{U}_{n+1}, \Delta t) = \frac{1}{\Delta t} \mathbf{M}(\mathbf{U}_{n+1} - \mathbf{U}_n) \quad (27)$$

where:

$$\frac{1}{\Delta t} (\mathbf{U}_{n+2} - \mathbf{U}_{n+1}) = \mathbf{V}_{n+3/2} \quad (28)$$

For the Lagrangian defined in (19), the discrete Euler-Lagrange equations lead to the central difference scheme [2, 7]:

$$\mathbf{M} \frac{\mathbf{U}_{n+2} - 2\mathbf{U}_{n+1} + \mathbf{U}_n}{\Delta t^2} = -\nabla P(\mathbf{U}_{n+1}) \quad (29)$$

$$\Leftrightarrow \mathbf{M}(\mathbf{V}_{n+3/2} - \mathbf{V}_{n+1/2}) = \Delta t (\mathbf{F}^{\text{ext}}(t_{n+1}) - \mathbf{F}^{\text{int}}_{n+1}) \quad (30)$$

The stability analysis of the scheme in the elastic case gives the critical time step  $\Delta t_{\text{cr}}^e = 2/\omega$  where  $\omega$  is the maximum frequency of the system. The mass matrix  $\mathbf{M}$  is lumped ensuring the discrete balance of mass, so that the resolution is matrix-free [12, 9]; it also provides a lower maximum frequency (then a higher critical time step) than a consistent mass matrix.

The following step is to express the internal nodal forces while maintaining an explicit scheme. In other words, this means that the internal force must depend on fields evaluated before  $t_{n+3/2}$ . The elastic contribution is given by  $\mathbf{K}\mathbf{U}_{n+1}$ , causing no problem. However, a direct integration of the time-discrete viscous strain-stress relationship:

$$\boldsymbol{\sigma}_{n+1}^v = (\eta \mathbb{I}) : \dot{\boldsymbol{\epsilon}}(\mathbf{u}_{n+1}) \quad (31)$$

with  $\dot{\boldsymbol{\epsilon}}(\mathbf{u}_{n+1}) = \boldsymbol{\epsilon}(\mathbf{v}_{n+1})$ , leads to the following expression for the internal nodal forces:

$$(F^{\text{int}})_{n+1}^i = \sum_{j=0}^{N_{\text{nodes}}} \left( K^{ij} u_{n+1}^j + v_{n+1}^j \underbrace{\int_{\Omega} \eta \mathbb{I} : \boldsymbol{\epsilon}(\mathbf{s}^i(\mathbf{x})) : \boldsymbol{\epsilon}(\mathbf{s}^j(\mathbf{x})) d\Omega}_{C^{ij}} \right) \quad (32)$$

$$\Rightarrow \mathbf{F}_{n+1}^{\text{int}} = \mathbf{K}\mathbf{U}_{n+1} + \mathbf{C}\mathbf{V}_{n+1} \quad (33)$$

with  $\mathbf{C}$  the viscous damping matrix, with components  $C^{ij}$ . Given that  $\mathbf{V}_{n+1} = (\mathbf{V}_{n+3/2} + \mathbf{V}_{n+1/2})/2$ , this direct integration leads to an implicit scheme. To address this issue, Belytschko [2] introduces a lag of a half time step within velocities in the calculation of internal viscous nodal force:

$$\boldsymbol{\sigma}_{n+1}^v = \eta \mathbb{I} : \boldsymbol{\epsilon}(\mathbf{v}_{n+1/2}) \quad (34)$$

which leads to the classical central difference scheme for transient dynamics of viscoelastic materials (with  $\mathbf{F}_{n+1}^{\text{int}} = \mathbf{K}\mathbf{U}_{n+1} + \mathbf{C}\mathbf{V}_{n+1/2}$ ).

### 3.2 The new $\alpha$ viscous stress averaging scheme

To improve the previous approximation (34), we propose a viscous stress-averaging method around  $t_{n+1/2}$ , by introducing a new parameter  $\alpha \in \mathbb{R}^+$ :

$$(1 - \alpha)\boldsymbol{\sigma}_n^v + \alpha\boldsymbol{\sigma}_{n+1}^v = \eta\mathbb{I} : \boldsymbol{\epsilon}(\mathbf{v}_{n+1/2}) \quad (35)$$

The internal nodal force vector becomes:

$$\begin{aligned} (\mathbf{F}^{\text{int}})_n^i &= \sum_{j=0}^{N_{\text{nodes}}} \left( K^{ij} u_{n+1}^j + \alpha^{-1} C^{ij} v_{n+1/2}^j - \alpha^{-1}(1 - \alpha) \int_{\Omega} \boldsymbol{\sigma}_n^v : \boldsymbol{\epsilon}(\mathbf{s}^i(\mathbf{x})) d\Omega \right) \\ \Rightarrow \mathbf{F}_{n+1}^{\text{int}} &= \mathbf{K}\mathbf{U}_{n+1} + \alpha^{-1} \mathbf{C}\mathbf{V}_{n+1/2} - \alpha^{-1}(1 - \alpha) \mathbf{F}^v(\boldsymbol{\sigma}_n^v) \end{aligned} \quad (36)$$

This integration method of the viscous stress strain law keeps the scheme explicit. Setting  $\alpha = 1$  leads to the approximation (34). We can quickly verify that the proposed approximation does not add any non physical term into the original problem. For an infinitesimal time step  $\boldsymbol{\sigma}_n \approx \boldsymbol{\sigma}$ ,  $\mathbf{v}_n \approx \mathbf{v}$ , we have, at the limit:

$$\lim_{\Delta t \rightarrow 0} (1 - \alpha)\boldsymbol{\sigma}_n^v + \alpha\boldsymbol{\sigma}_{n+1}^v - \eta\mathbb{I} : \boldsymbol{\epsilon}(\mathbf{v}_{n+1/2}) = \boldsymbol{\sigma}^v - \eta\mathbb{I} : \boldsymbol{\epsilon}(\mathbf{v}) \quad (37)$$

which is exactly the physical problem to be solved. Then, the system of equations to integrate is the following:

$$\begin{aligned} \mathbf{U}_{n+1} &= \mathbf{U}_n + \Delta t \mathbf{V}_{n+1/2} && \text{(Displacement update)} \\ \boldsymbol{\sigma}_{n+1}^v &= \alpha^{-1} \eta \mathbb{I} : \boldsymbol{\epsilon}(\mathbf{v}_{n+1/2}) - \alpha^{-1}(1 - \alpha) \boldsymbol{\sigma}_n^v && \text{(Viscous strain integration)} \\ \mathbf{F}_{n+1}^{\text{int}} &= \mathbf{K}\mathbf{U}_{n+1} + \mathbf{F}^v(\boldsymbol{\sigma}_{n+1}^v) && \text{(Internal nodal force)} \\ \mathbf{M}(\mathbf{V}_{n+3/2} - \mathbf{V}_{n+1/2}) &= \Delta t(\mathbf{F}^{\text{ext}}(t_{n+1}) - \mathbf{F}_{n+1}^{\text{int}}) && \text{(Dynamic equation)} \end{aligned} \quad (38)$$

which implementation is presented in Algorithm 1.

---

#### Algorithm 1 Central difference scheme with $\alpha$ viscous stress averaging procedure

---

```

Input :  $\mathbf{M}, \mathbf{C}, \mathbf{K}, \mathbf{F}^{\text{ext}}(t), \mathbf{U}_0, \mathbf{V}_0, \boldsymbol{\sigma}_0^v, \alpha$ 
 $\mathbf{F}_0^{\text{int}} = \mathbf{K}\mathbf{U}_0 + \alpha^{-1}(\mathbf{C}\mathbf{V}_0 - \Delta t(1 - \alpha)\mathbf{F}^v(\boldsymbol{\sigma}_0^v))$ 
Solve  $\mathbf{M}(\mathbf{V}_{1/2} - \mathbf{V}_0) = \Delta t(\mathbf{F}^{\text{ext}}(t_0) - \mathbf{F}_0^{\text{int}})$  to get  $\mathbf{V}_{1/2}$ 
while  $n + 1 \leq N_t$  do
     $\mathbf{U}_{n+1} = \mathbf{U}_n + \Delta t \mathbf{V}_{n+1/2}$ 
     $\boldsymbol{\sigma}_{n+1}^v = \alpha^{-1} \eta \mathbb{I} : \boldsymbol{\epsilon}(\mathbf{v}_{n+1/2}) - \alpha^{-1}(1 - \alpha) \boldsymbol{\sigma}_n^v$ 
     $\mathbf{F}_{n+1}^{\text{int}} = \mathbf{K}\mathbf{U}_{n+1} + \mathbf{F}^v(\boldsymbol{\sigma}_{n+1}^v)$ 
    Solve  $\mathbf{M}(\mathbf{V}_{n+3/2} - \mathbf{V}_{n+1/2}) = \Delta t(\mathbf{F}^{\text{ext}}(t_{n+1}) - \mathbf{F}_{n+1}^{\text{int}})$  to get  $\mathbf{V}_{n+3/2}$ 
    Increment  $n$ 
end while

```

---

We perform a stability analysis of the method, based on a spectral stability criterion. The amplification matrix  $\mathbf{A}(\Delta t, \alpha)$  of the method links two consecutive state vectors as

$$\begin{pmatrix} \mathbf{V}_{n+3/2} \\ \mathbf{U}_{n+1} \\ \boldsymbol{\sigma}_{n+1} \end{pmatrix} = \mathbf{A}(\Delta t, \alpha) \begin{pmatrix} \mathbf{V}_{n+1/2} \\ \mathbf{U}_n \\ \boldsymbol{\sigma}_n \end{pmatrix} \quad (39)$$

The scheme is said to be stable if the spectral radius of the amplification matrix remains below one [12].

Examples and applications are presented for the case of an unidimensional beam. In this case, strains and stress become vectors, which lets us define  $\mathbf{B}_\varepsilon^i$  the elementary strain nodal displacement vector,  $\mathbf{B}_\varepsilon$  the strain nodal displacement matrix, and  $\mathbf{B}_\sigma$  as:

$$\boldsymbol{\epsilon}(\mathbf{U}_{n+1}) = \mathbf{B}_\varepsilon \mathbf{U}_{n+1} \quad (40)$$

$$\int_{\Omega} \boldsymbol{\sigma} : \boldsymbol{\epsilon}(\mathbf{u}^*) d\Omega = \sum_{i=0}^{N_{\text{nodes}}} (u^*)^i(t) \int_{\Omega} \mathbf{B}_\varepsilon^{i\top} \boldsymbol{\sigma} d\Omega = \mathbf{U}^* \cdot (\mathbf{B}_\sigma^\top \boldsymbol{\sigma}) \quad (41)$$

The amplification matrix for this problem is:

$$\mathbf{A}(\Delta t, \alpha) = \begin{pmatrix} \mathbf{M} & \Delta t \mathbf{K} & \mathbf{0} \\ \mathbf{0} & \mathbf{Id} & \mathbf{0} \\ \mathbf{0} & -E\mathbf{B}_\varepsilon & \mathbf{Id} \end{pmatrix}^{-1} \begin{pmatrix} \mathbf{M} - \Delta t \alpha^{-1} \mathbf{C} - \Delta t \alpha^{-1} (1 - \alpha) \mathbf{K} & \Delta t \alpha^{-1} (1 - \alpha) \mathbf{B}_\sigma^\top \\ \Delta t \mathbf{Id} & \mathbf{Id} & \mathbf{0} \\ \alpha^{-1} \eta \mathbf{B}_\varepsilon & \alpha^{-1} (1 - \alpha) E \mathbf{B}_\varepsilon & -\alpha^{-1} (1 - \alpha) \mathbf{Id} \end{pmatrix} \quad (42)$$

This expression of the amplification matrix further motivates our choice of state vector. Previous studies, such as the approximation presented by Belytschko, perform spectral stability analysis using a state vector composed only of the velocity and displacement fields. However, the amplification matrix reveals that setting  $\alpha = 1$  results in a null eigenvalue on the stress component of the amplification matrix. This indicates that the stress was not relevant within the state vector of Belytschko's approximation stability analysis, while it is in our analysis.

Material properties of the beam, made of ABS [13] are summarized in Table 1. Different viscosity parameters ( $\eta = 2.09 \times 10^{-2}$  MPa s,  $\eta = 2.46 \times 10^{-2}$  MPa s,  $\eta = 3.05 \times 10^{-2}$  MPa s,  $\eta = 3.89 \times 10^{-2}$  MPa s) are used through the following applications. Moreover, to monitor the impact of highly viscously damped materials on the scheme, we introduce non physical virtual high viscosity parameters.

Length $L$	Section $S$	Density $\rho$	Young modulus $E$	Number of nodes $N_{\text{nodes}}$
1000 mm	100 mm <sup>2</sup>	$1.05 \times 10^4$ kg m <sup>-3</sup>	880 MPa	21

Table 1: Material properties and geometry of the considered unidimensional beam.

For a given material, and a spatial discretization, we can vary  $\alpha$  to change the critical time step. For this beam, in the elastic case, the critical time step is given as  $\Delta t_{\text{cr}}^e = \Delta x \sqrt{\rho/E} = 1.73 \times 10^{-2}$  s. Figure 1 displays the evolution of the critical time step as a function of  $\alpha$  for different viscosities. For  $\alpha < 1/2$ , the scheme is

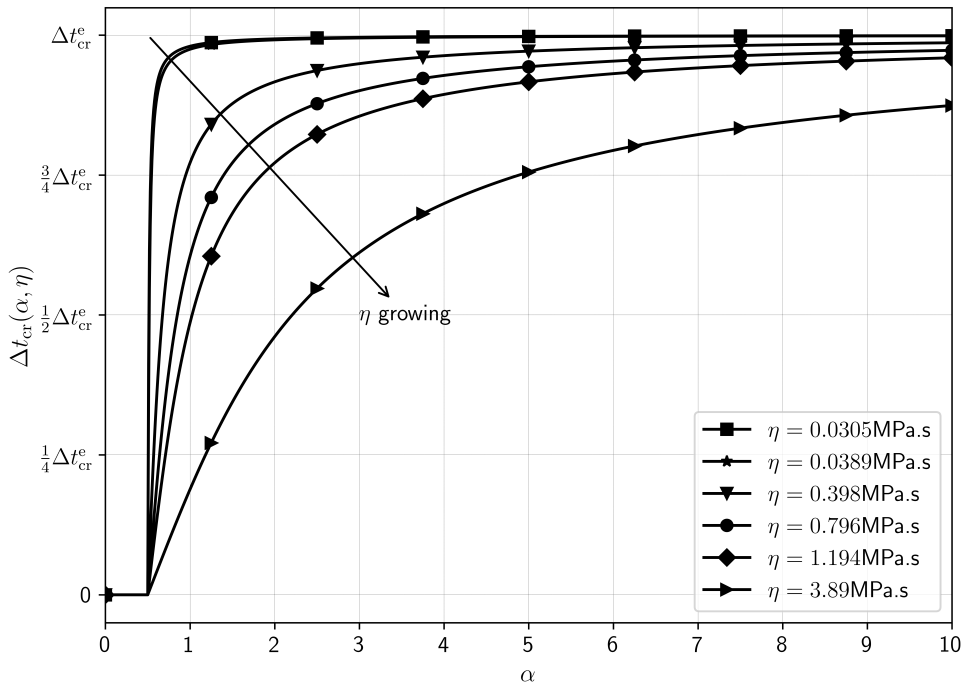


Fig. 1: Critical time step as a function of  $\alpha$ , for different viscosities (see table 1 for the material properties).

unconditionally unstable. For  $\alpha \rightarrow \infty$ , the critical time step tends towards the elastic one ( $\Delta t_{\text{cr}}^e$ ). Indeed:

$$((1 - \alpha)\boldsymbol{\sigma}_n^v + \alpha\boldsymbol{\sigma}_{n+1}^v - \eta\mathbb{I} : \boldsymbol{\varepsilon}(\boldsymbol{v}_{n+1/2})) \underset{\alpha \rightarrow +\infty}{\sim} \alpha(\boldsymbol{\sigma}_{n+1}^v - \boldsymbol{\sigma}_n^v) \quad (43)$$

meaning that viscous strains remain constant during the integration for infinite  $\alpha$ . Highly viscous damped material seems to have wider ranges of critical time step improvement. To assess the relevance of this method, we observe the maximum error made by the simulation on its critical time step, when compared with a time refined solution (calculated with  $\alpha = 1$ ,  $\Delta t = \Delta t_{\text{cr}}(\alpha = 1, \eta) \times 10^{-3}$ ). Refined and simulated displacements are denoted respectively  $\boldsymbol{U}_{\text{ex}}$  and  $\boldsymbol{U}_{\text{sim}}$ . Then, the error in displacement, calculated at the center of the beam, is quantified, as:

$$e_\infty = \frac{\|\boldsymbol{U}_{\text{sim}} - \boldsymbol{U}_{\text{ex}}\|_\infty}{\|\boldsymbol{U}_{\text{ex}}\|_\infty} = \max_{t \in [t_0, t_f]} \frac{|\boldsymbol{U}_{\text{sim}}(t) - \boldsymbol{U}_{\text{ex}}(t)|}{|\boldsymbol{U}_{\text{ex}}(t)|} \quad (44)$$

Figure 2 represents, for the beam (table 1) with different viscosity parameters, the time step gain as a function of the error  $e_\infty$ , for different values of  $\alpha$ . Dotted lines represent iso- $\alpha$  curves.

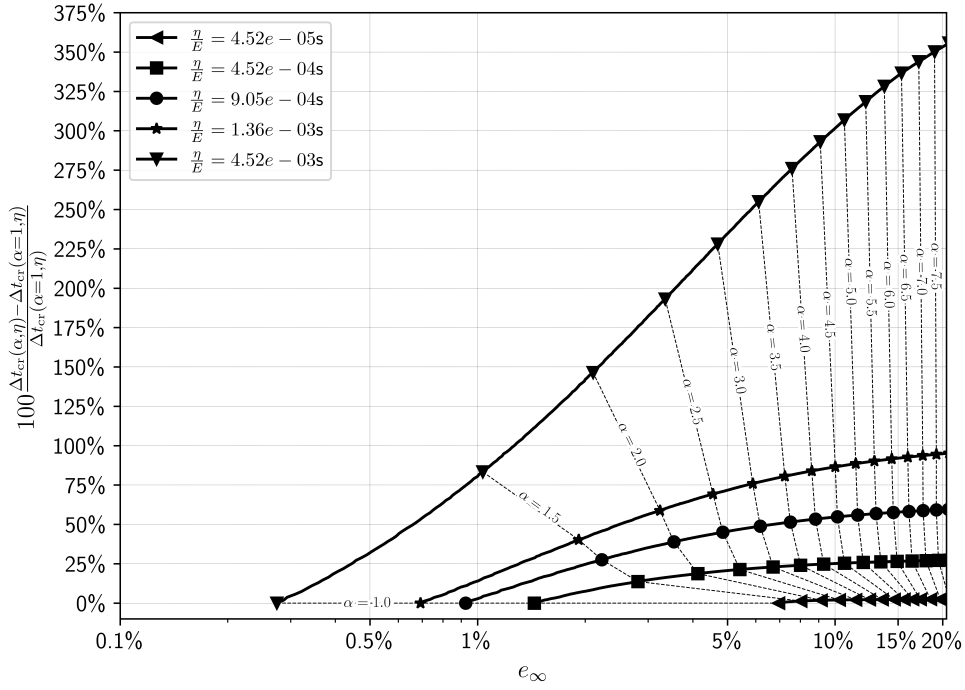


Fig. 2: Critical time step gain versus error for different values of  $\eta$  and  $\alpha$ .

We can draw the following observations from the analysis of the previous figure. For small values of viscosity  $\eta/E \approx 1 \times 10^{-5}$  s, the critical time step is not increased by more than 2%, while, for higher viscosity values, there is a significant increase of the stability limit. For a highly viscous material, e.g., for  $\eta/E = 4.52 \times 10^{-3}$  s and  $\alpha = 3$ , the critical time step increases by 225% compared to the previous known approximation ( $\alpha = 1$ ), with the infinite norm error remaining below 4%. Therefore, this method augments substantially the critical time step for highly viscously damped materials. Finally, we should note that the error seems to grow dramatically for higher values of  $\alpha$ , thus making the analysis combining accuracy and stability criteria important to choose the parameter  $\alpha$ .

#### 4 Variable time step

We now consider a variable time step  $\Delta t_{n+1} = t_{n+1} - t_n$ . As discussed in the introduction, previous studies have demonstrated that variable time step can introduce numerical instability in the central difference method. Therefore, to compare our results with these specific studies, the former finite element approximation is reduced to a single degree of freedom problem (a spring-damped-mass system). The mass is denoted  $m$ , the stiffness of the spring  $k$ , and the viscous damping parameter  $c$ . For the numerical implementation, these parameters are calculated thanks to previous values of Young modulus, density, section and length (see Table 1) as  $m = \rho S L = 1.05 \times 10^{-1}$  kg,  $k = E S / L = 88$  N mm $^{-1}$  and  $c = \eta S / L$ . Displacement, velocity and acceleration are respectively denoted by  $u$ ,  $v$  and  $a$ .

##### 4.1 Preliminary results

*Expression of the variable time step central difference scheme* We start with the Newmark's scheme for the central difference method

$$v_{n+1} = v_n + \frac{\Delta t}{2} (a_n + a_{n+1}) \quad (45)$$

$$u_{n+1} = u_n + \Delta t_{n+1} v_n + \frac{\Delta t^2}{2} a_n \quad (46)$$

By taking both of these relationships, we can formulate the multistep form of the central difference equation for variable time steps:

$$m \frac{\Delta t_{n+1}(u_{n+2} - u_{n+1}) - \Delta t_{n+2}(u_{n+1} - u_n)}{\Delta t_{n+2}\Delta t_{n+1}} = \frac{1}{2} (\Delta t_{n+2} + \Delta t_{n+1})(F_{n+1}^{\text{ext}} - F_{n+1}^{\text{int}}) \quad (47)$$

which gives in terms of the half step velocities

$$m(v_{n+3/2} - v_{n+1/2}) = \frac{1}{2}(\Delta t_{n+2} + \Delta t_{n+1})(F_{n+1}^{\text{ext}} - F_{n+1}^{\text{int}}) \quad (48)$$

where

$$v_{n+1/2} = \frac{1}{\Delta t_{n+1}}(u_{n+1} - u_n) \quad (49)$$

In the elastic case, internal forces will be considered as:

$$F_{n+1}^{\text{int}} = ku_{n+1} \quad (50)$$

In the viscoelastic case, the half lagged velocity approximation will be considered:

$$F_{n+1}^{\text{int}} = ku_{n+1} + cv_{n+1/2} \quad (51)$$

introduced by Belytschko [2].

*Energy balance* In both elastic and viscoelastic test cases, we will compute the energy balance of the method, as an indicator of potential instability. While the energy balance for constant time steps has been extensively studied [9, 17], it has not been explored in the context of variable time step framework.

**Proposition 1** *The energy balance of the central difference method, in the case of a viscoelastic 0D problem, with the half lagged velocity approximation on the viscous force is, with  $[u]_n^{n+1} = u_{n+1} - u_n$ :*

$$\begin{aligned} & \left[ \frac{1}{2}mv^2 + \frac{1}{2}ku^2 \right]_n^{n+1} - \frac{\Delta t_{n+1}^2}{4} \left[ \frac{1}{2}ma^2 \right]_n^{n+1} \\ &= -\frac{1}{2} \frac{1}{\Delta t_{n+1}} c(u_{n+1} - u_n)^2 - \frac{1}{2} \frac{1}{\Delta t_n} c(u_{n+1} - u_n)(u_n - u_{n-1}) \end{aligned} \quad (52)$$

Between  $t_n$  and  $t_{n+2}$ , the energy balance is:

$$\begin{aligned} & \left[ \frac{1}{2}mv^2 + \frac{1}{2}ku^2 \right]_n^{n+2} - \frac{\Delta t_{n+1}^2}{4} \left[ \frac{1}{2}ma^2 \right]_n^{n+1} - \frac{\Delta t_{n+2}^2}{4} \left[ \frac{1}{2}ma^2 \right]_{n+1}^{n+2} \\ &= -\frac{1}{2} \frac{1}{\Delta t_{n+2}} c(u_{n+2} - u_{n+1})^2 + \\ & - \frac{1}{2} \frac{1}{\Delta t_{n+1}} c(u_{n+1} - u_n)^2 - \frac{1}{2} \frac{1}{\Delta t_{n+1}} c(u_{n+2} - u_{n+1})(u_{n+1} - u_n) + \\ & - \frac{1}{2} \frac{1}{\Delta t_n} c(u_{n+1} - u_n)(u_n - u_{n-1}) \end{aligned} \quad (53)$$

*Proof* We first express the central difference equation as introduced by Newmark [21], defining the mean  $\langle u \rangle_n^{n+1} = \frac{1}{2}(u_{n+1} + u_n)$  and the difference operator  $[u]_n^{n+1} = (u_{n+1} - u_n)$ :

$$[v]_n^{n+1} = \Delta t_{n+1} \langle a \rangle_n^{n+1} \quad (54)$$

$$[u]_n^{n+1} = \Delta t_{n+1} \langle v \rangle_n^{n+1} - \frac{1}{4} \Delta t_{n+1}^2 [a]_n^{n+1} \quad (55)$$

Then, the kinetic energy balance equation leads to, knowing that  $ma_{n+1} = -ku_{n+1} - cv_{n+1/2}$ :

$$\begin{aligned} \left[ \frac{1}{2}mv^2 \right]_n^{n+1} &= \langle v \rangle_n^{n+1} m [v]_n^{n+1} \\ &= \langle a \rangle_n^{n+1} m ([u]_n^{n+1} + \frac{1}{4} \Delta t_{n+1}^2 [a]_n^{n+1}) \\ &= -\langle u \rangle_n^{n+1} k [u]_n^{n+1} + \frac{1}{4} \Delta t_{n+1}^2 \langle a \rangle_n^{n+1} m [a]_n^{n+1} + \\ & - \frac{1}{2} \frac{1}{\Delta t_{n+1}} c(u_{n+1} - u_n)(u_{n+1} - u_n) - \frac{1}{2} \frac{1}{\Delta t_n} c(u_{n+1} - u_n)(u_n - u_{n-1}) \end{aligned} \quad (56)$$

When summed with the kinetic energy balance between  $t_{n+2}$  and  $t_{n+1}$ , one obtains equation (53).

The following subsection develops, in the elastic and the viscoelastic cases, the stability analysis of the variable time step central difference scheme.

## 4.2 Stability analysis

The central difference method can be formulated in three different ways. The first, denoted by ①, is based on half step velocities as described in equation (48). The second formulation, denoted by ②, is a one step approach based on the Newmark integration method, examined in Wright's [27] and Skeel's [24] studies. The third formulation, denoted by ③, is a multistep approach, where "multistep" refers to the method's dependence only on the displacement field, as depicted in equation (47).

We now perform a stability analysis of each formulation, which will show that the spectral stability criteria gives different results for each of the formulation. State vectors will consist of velocity and displacement, on a suitable time step ensuring that the analyses are lead on the same time intervals. Therefore, we will define the stability boundaries of two subsequent time steps ( $\Delta t_{n+2}, \Delta t_{n+1}$ ) such that the method remains spectrally stable.

Since the amplification matrices will be of size  $2 \times 2$ , we can study its invariants to compute the exact bounds of the stability regions. With  $\mathbf{A}$  the amplification matrix, the method is stable, and has an oscillating behaviour, if [12,9]:

$$1 + \det(\mathbf{A}) \geq 0 \quad (57)$$

$$1 - \det(\mathbf{A}) \geq 0 \quad (58)$$

$$1 + \det(\mathbf{A}) + \text{tr}(\mathbf{A}) \geq 0 \quad (59)$$

$$1 + \det(\mathbf{A}) - \text{tr}(\mathbf{A}) \geq 0 \quad (60)$$

$$\text{tr}^2(\mathbf{A}) - 4 \det(\mathbf{A}) < 0 \quad (61)$$

### 4.2.1 The elastic case

First, we consider the elastic case, turning the dynamic equation to the classical wave equation:

$$\frac{dv}{dt} = -\frac{k}{m}u \quad (62)$$

*Half step formula ①* This first method is defined as [2,7]:

$$u_{n+1} = u_n + \Delta t_{n+1} v_{n+1/2} \quad (63)$$

$$m(v_{n+3/2} - v_{n+1/2}) = -k \frac{\Delta t_{n+2} + \Delta t_{n+1}}{2} u_{n+1} \quad (64)$$

The equations depends on two consecutive time steps. We can therefore directly perform the stability analysis of the method with the amplification matrix

$$\begin{pmatrix} v_{n+3/2} \\ u_{n+1} \end{pmatrix} = \mathbf{A}^{\circledast}(\Delta t_{n+2}, \Delta t_{n+1}) \begin{pmatrix} v_{n+1/2} \\ u_n \end{pmatrix} \quad (65)$$

defined by

$$\mathbf{A}^{\circledast}(\Delta t_{n+2}, \Delta t_{n+1}) = \begin{pmatrix} A_{11} & A_{12} \\ A_{21} & A_{22} \end{pmatrix} \quad (66)$$

$$A_{11} = 1 - \frac{1}{2} \Delta t_{n+1} (\Delta t_{n+2} + \Delta t_{n+1}) \frac{k}{m} \quad (67)$$

$$A_{12} = -\frac{1}{2} (\Delta t_{n+2} + \Delta t_{n+1}) \frac{k}{m} \quad (68)$$

$$A_{21} = \Delta t_{n+1} \quad (69)$$

$$A_{22} = 1 \quad (70)$$

**Proposition 2** *The analysis of the amplification matrix defined by the half step formulation of the central difference method leads to the following stability condition on time steps:*

$$4 - \frac{1}{2} \Delta t_{n+1} (\Delta t_{n+2} + \Delta t_{n+1}) \frac{k}{m} \geq 0 \quad (71)$$

*Proof* Only the condition  $1 + \det(\mathbf{A}^{\circledast}) + \text{tr}(\mathbf{A}^{\circledast}) \geq 0$  is not true for all  $\Delta t_{n+2}, \Delta t_{n+1}$ , giving the condition (71).

The condition (71) is always true below the critical time step  $\Delta t_{\text{cr}}^{\text{e}} = 2/\omega$  with  $\omega = \sqrt{k/m}$ . Hence, this stability analysis states that there is no condition on the evolution of time steps below this critical time step.

*One step formulation ②* This formulation is analysed in [24, 27], and is defined as:

$$v_{n+1} = v_n + \frac{1}{2} \Delta t_{n+1} (a_n + a_{n+1}) \quad (72)$$

$$u_{n+1} = u_n + \Delta t_{n+1} v_n + \frac{1}{2} \Delta t_{n+1}^2 a_n \quad (73)$$

$$a_{n+1} = -\frac{k}{m} u_{n+1} \quad (74)$$

Analysis on a single amplification matrix on one time step leads to the condition  $\Delta t_{n+1} \leq \Delta t_{cr}^e$ . It is then required to extend the analysis to two consecutive time steps, to be able to monitor how variable time stepping affects the method:

$$\begin{aligned} \begin{pmatrix} v_{n+2} \\ u_{n+2} \end{pmatrix} &= \mathbf{A}^{\circledast}(\Delta t_{n+2}) \mathbf{A}^{\circledast}(\Delta t_{n+1}) \begin{pmatrix} v_n \\ u_n \end{pmatrix} \\ \iff \begin{pmatrix} v_{n+2} \\ u_{n+2} \end{pmatrix} &= \mathbf{A}^{\circledast}(\Delta t_{n+2}, \Delta t_{n+1}) \begin{pmatrix} v_n \\ u_n \end{pmatrix} \end{aligned} \quad (75)$$

The amplification matrix is:

$$\mathbf{A}^{\circledast}(\Delta t_{n+2}, \Delta t_{n+1}) = \begin{pmatrix} A_{11} & A_{12} \\ A_{21} & A_{22} \end{pmatrix} \quad (76)$$

$$A_{11} = (1 - \frac{1}{2} \Delta t_{n+1}^2 \frac{k}{m})(1 - \frac{1}{2} \Delta t_{n+2}^2 \frac{k}{m}) + \Delta t_{n+1} \Delta t_{n+2} \frac{k}{m} (-1 + \frac{1}{4} \Delta t_{n+2}^2 \frac{k}{m}) \quad (77)$$

$$A_{12} = (1 - \frac{1}{2} \Delta t_{n+2}^2 \frac{k}{m}) \Delta t_{n+1} \frac{k}{m} (-1 + \frac{1}{4} \Delta t_{n+1}^2 \frac{k}{m}) + \quad (78)$$

$$+ (1 - \frac{1}{2} \Delta t_{n+1}^2 \frac{k}{m}) \Delta t_{n+2} \frac{k}{m} (-1 + \frac{1}{4} \Delta t_{n+2}^2 \frac{k}{m}) \quad (79)$$

$$A_{21} = \Delta t_{n+1} (1 - \frac{1}{2} \Delta t_{n+2}^2 \frac{k}{m}) + \Delta t_{n+2} (1 - \frac{1}{2} \Delta t_{n+1}^2 \frac{k}{m}) \quad (80)$$

$$A_{22} = (1 - \frac{1}{2} \Delta t_{n+1}^2 \frac{k}{m})(1 - \frac{1}{2} \Delta t_{n+2}^2 \frac{k}{m}) + \Delta t_{n+1} \Delta t_{n+2} \frac{k}{m} (-1 + \frac{1}{4} \Delta t_{n+1}^2 \frac{k}{m}) \quad (81)$$

Studying the invariants of the amplification matrix [12, 2] leads to the two following conditions:

$$(\Delta t_{n+2} + \Delta t_{n+1})^2 (1 - \frac{1}{4} \frac{k}{m} \Delta t_{n+2} \Delta t_{n+1}) \geq 0 \quad (82)$$

$$2 - (\Delta t_{n+2} + \Delta t_{n+1})^2 (1 - \frac{1}{4} \frac{k}{m} \Delta t_{n+2} \Delta t_{n+1}) \geq 0 \quad (83)$$

both stated in [27]. These conditions create instability zones of  $(\Delta t_{n+2}, \Delta t_{n+1})$ , for which the method may become unstable despite time steps being below the critical time step  $\Delta t_{cr}^e$ .

*Multistep formulation ③* Finally, the last equation is the multistep formulation:

$$m u_{n+2} - \frac{\Delta t_{n+2} + \Delta t_{n+1}}{\Delta t_{n+1}} m u_{n+1} + \frac{\Delta t_{n+2}}{\Delta t_{n+1}} m u_n = -\frac{1}{2} (\Delta t_{n+2} + \Delta t_{n+1}) \Delta t_{n+2} \frac{k}{m} u_{n+1} \quad (84)$$

The amplification matrix given by this approximation is:

$$\begin{pmatrix} u_{n+2} \\ u_{n+1} \end{pmatrix} = \mathbf{A}^{\circledast}(\Delta t_{n+2}, \Delta t_{n+1}) \begin{pmatrix} u_{n+1} \\ u_n \end{pmatrix} \quad (85)$$

with

$$\mathbf{A}^{\circledast}(\Delta t_{n+2}, \Delta t_{n+1}) = \begin{pmatrix} A_{11} & A_{12} \\ A_{21} & A_{22} \end{pmatrix} \quad (86)$$

$$A_{11} = \frac{1}{\Delta t_{n+1}} (\Delta t_{n+2} + \Delta t_{n+1}) (1 - \frac{1}{2} \Delta t_{n+2} \Delta t_{n+1}) \quad (87)$$

$$A_{12} = -\frac{\Delta t_{n+2}}{\Delta t_{n+1}} \quad (88)$$

$$A_{21} = 1 \quad (89)$$

$$A_{22} = 0 \quad (90)$$

The analysis of the amplification matrix leads to the following propositions.

**Proposition 3** *The characteristic polynomial of the amplification matrix  $\mathbf{A}^{\circledast}$  is exactly equal to the generating polynomial of the linear multistep method:*

$$\theta(\zeta) = \zeta^2 + \frac{\Delta t_{n+2} + \Delta t_{n+1}}{\Delta t_{n+1}} \left( -1 + \frac{1}{2} \Delta t_{n+2} \Delta t_{n+1} \frac{k}{m} \right) \zeta + \frac{\Delta t_{n+2}}{\Delta t_{n+1}} \quad (90)$$

introduced by Dahlquist [6].

*Proof* The terms of the characteristic polynomial, determined by  $\det(\mathbf{A}^{\circledast} - \zeta \mathbf{Id})$  can be identified one by one to the terms of the generating polynomial of the linear multistep method.

The generating polynomial is used to assess the zero-stability of the scheme [6, 11]. Then, as stated in the proposition below, the study of the roots of the polynomial in equation (90) is equivalent to the study of the matrix norm of  $\mathbf{A}^{\circledast}$ , hence its spectral radius. This study is lead in the following proposition.

**Proposition 4** *The analysis of the amplification matrix defined by the multistep formulation leads to the following conditions:*

$$\Delta t_{n+2} \Delta t_{n+1} \leq (\Delta t_{cr}^e)^2 \quad (91)$$

$$\Delta t_{n+2} \leq \Delta t_{n+1} \quad (92)$$

$$(\Delta t_{n+2} + \Delta t_{n+1})^2 \left( 1 - \frac{1}{2} \Delta t_{n+2} \Delta t_{n+1} \frac{k}{m} \right)^2 - 4 \Delta t_{n+1} \Delta t_n < 0 \quad (93)$$

*Proof* Condition (91) is given by:

$$1 + \det(\mathbf{A}^{\circledast}) + \text{tr}(\mathbf{A}^{\circledast}) \geq 0 \Leftrightarrow (\Delta t_{n+2} + \Delta t_{n+1}) \left( 2 - \frac{1}{2} \Delta t_{n+2} \Delta t_{n+1} \frac{k}{m} \right) \geq 0 \quad (94)$$

$$\Leftrightarrow \Delta t_{n+2} \Delta t_{n+1} \leq (\Delta t_{cr}^e)^2 \quad (95)$$

Condition (92) is given by  $1 - \det(\mathbf{A}^{\circledast}) \geq 0$ . Finally, the last condition (93) is obtained through  $\text{tr}^2(\mathbf{A}^{\circledast}) - 4 \det(\mathbf{A}^{\circledast}) < 0$ . Other conditions ( $1 + \det(\mathbf{A}^{\circledast}) \geq 0, 1 + \det(\mathbf{A}^{\circledast}) - \text{tr}(\mathbf{A}^{\circledast}) \geq 0$ ) lead to inequalities always true for all  $\Delta t_{n+2}, \Delta t_{n+1}$ .

*Analysis and results* For each formulation of the central difference method (① half step, ② one step, ③ multistep), time step domains of  $(\Delta t_{n+2}, \Delta t_{n+1})$  satisfying their respective stability conditions, stated above, are plotted in Figure 3. The analysis is, in this particular figure, restricted to time steps inferior to the critical constant time step  $\Delta t_n \leq \Delta t_{cr}^e = 2/\omega$ .

As we can see in Figure 3, the analysis from the three different formulations differ from each other. First, below the critical time step, the half step analysis is not restrictive at all, allowing any change of time step during the integration. Indeed, equation (71) remains true for all  $\Delta t_n \leq \Delta t_{cr}^e$ . This statement goes in contradiction with the one step and the multistep analysis, in which unstable domains appear below  $\Delta t_{cr}^e$ . Second, the one step analysis leads to the same conclusions as Wright [27]: two unstable domains appear, with a bifurcation point corresponding to  $(\sqrt{2}/2)\Delta t_{cr}^e$ . The case  $\Delta t_{n+1} = \Delta t_{n+2}$  remains stable under  $\Delta t_{cr}^e$ . Finally, the multistep analysis is more restrictive, as stated in the analytical stability conditions. The time step cannot be increased during the simulation (see equation (92)) and an unstable zone appears below  $\Delta t_{cr}^e$  (see equation (93)). As stated by the analytical boundaries, the three analysis lead to three different stability domains, a phenomenon explained in the following proposition.

**Proposition 5** *The three formulations of the variable time step central difference method are not spectrally similar.*

*Proof* To prove the proposition, we express each state vector as a function of the other formulations, thanks to the following matrices:

$$\begin{pmatrix} v_{n+3/2} \\ u_{n+1} \end{pmatrix} = \mathbf{B}_{n+2} \begin{pmatrix} u_{n+2} \\ u_{n+1} \end{pmatrix} \text{ with } \mathbf{B}_{n+2} = \frac{1}{\Delta t_{n+2}} \begin{pmatrix} 1 & -1 \\ 0 & \Delta t_{n+2} \end{pmatrix} \quad (96)$$

$$\begin{pmatrix} v_{n+1} \\ u_{n+1} \end{pmatrix} = \mathbf{D}_{n+2} \begin{pmatrix} u_{n+2} \\ u_{n+1} \end{pmatrix} \text{ with } \mathbf{D}_{n+2} = \frac{1}{\Delta t_{n+2}} \begin{pmatrix} 1 - (1 - \frac{1}{2} \Delta t_{n+2} \frac{k}{m}) & 0 \\ 0 & \Delta t_{n+2} \end{pmatrix} \quad (97)$$

Since  $\det(\mathbf{B}_{n+2}) = \det(\mathbf{D}_{n+2}) = 1$ , the matrices can be inverted, and:

$$\begin{pmatrix} v_{n+1} \\ u_{n+1} \end{pmatrix} = \mathbf{D}_{n+2}^{-1} \mathbf{B}_{n+2}^{-1} \begin{pmatrix} v_{n+3/2} \\ u_{n+1} \end{pmatrix} \quad (98)$$

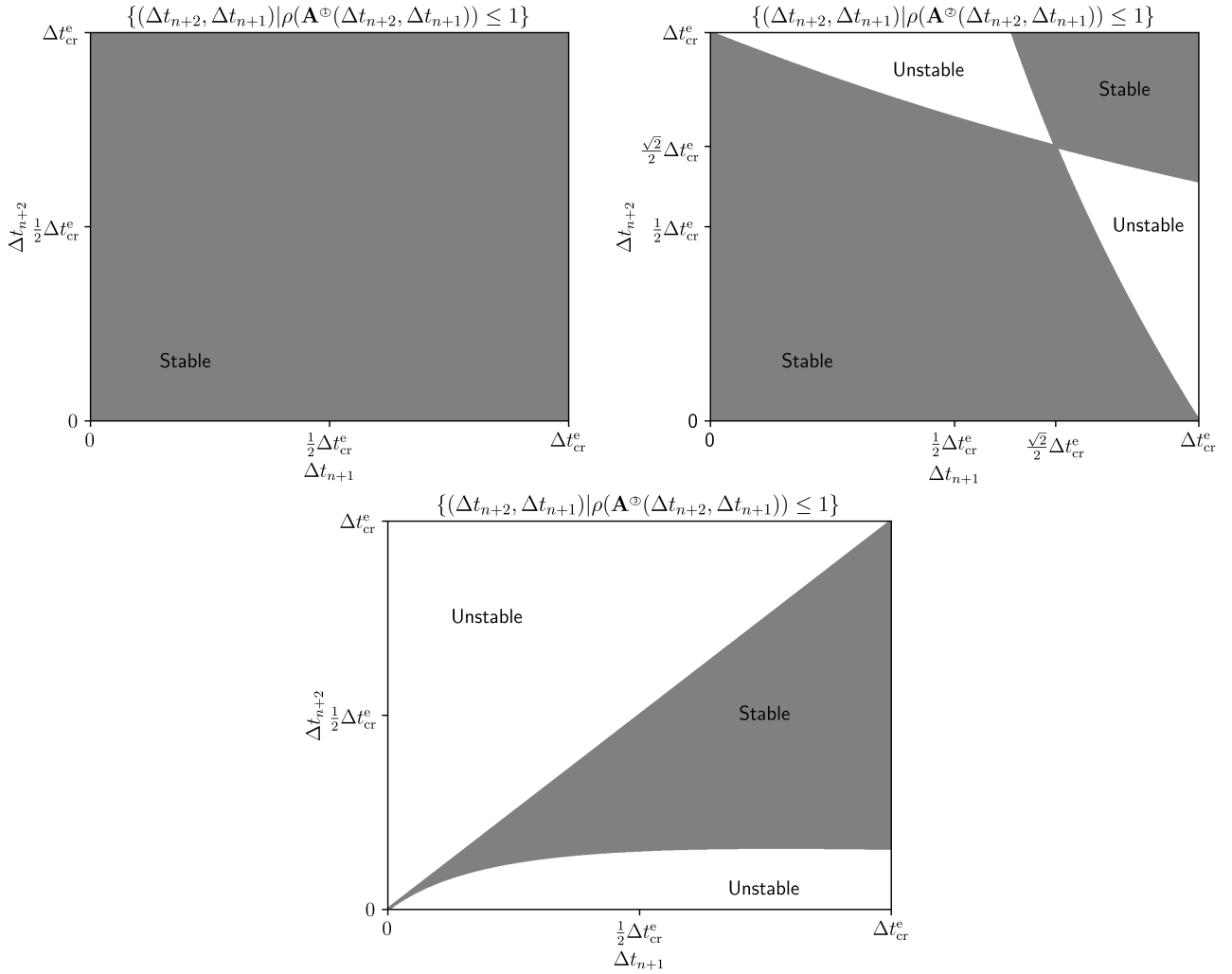


Fig. 3: Stable and unstable domains of  $(\Delta t_{n+2}, \Delta t_{n+1})$  for the three formulations, below  $\Delta t_{cr}^e$ .

We then compute the relationships between amplification matrices:

$$\textcircled{2} \rightarrow \textcircled{1} \begin{pmatrix} v_{n+3/2} \\ u_{n+1} \end{pmatrix} = (\mathbf{D}_{n+2}\mathbf{B}_{n+2}^{-1})^{-1}\mathbf{A}^{\textcircled{2}}(\Delta t_{n+2}, \Delta t_{n+1})(\mathbf{D}_{n+1}\mathbf{B}_{n+1}^{-1}) \begin{pmatrix} v_{n+1/2} \\ u_n \end{pmatrix} \quad (99)$$

$$\textcircled{3} \rightarrow \textcircled{2} \begin{pmatrix} v_{n+1} \\ u_{n+1} \end{pmatrix} = \mathbf{D}_{n+2}\mathbf{A}^{\textcircled{3}}(\Delta t_{n+2}, \Delta t_{n+1})\mathbf{D}_{n+1}^{-1} \begin{pmatrix} v_n \\ u_n \end{pmatrix} \quad (100)$$

$$\textcircled{1} \rightarrow \textcircled{3} \begin{pmatrix} u_{n+2} \\ u_{n+1} \end{pmatrix} = \mathbf{B}_{n+2}^{-1}\mathbf{A}^{\textcircled{1}}(\Delta t_{n+2}, \Delta t_{n+1})\mathbf{B}_{n+1} \begin{pmatrix} u_{n+1} \\ u_n \end{pmatrix} \quad (101)$$

which lead to the following equations:

$$\mathbf{A}^{\textcircled{1}} = (\mathbf{D}_{n+2}\mathbf{B}_{n+2}^{-1})^{-1}\mathbf{A}^{\textcircled{2}}(\Delta t_{n+2}, \Delta t_{n+1})(\mathbf{D}_{n+1}\mathbf{B}_{n+1}^{-1}) \quad (102)$$

$$\mathbf{A}^{\textcircled{2}} = \mathbf{D}_{n+2}\mathbf{A}^{\textcircled{3}}(\Delta t_{n+2}, \Delta t_{n+1})\mathbf{D}_{n+1}^{-1} \quad (103)$$

$$\mathbf{A}^{\textcircled{3}} = \mathbf{B}_{n+2}^{-1}\mathbf{A}^{\textcircled{1}}(\Delta t_{n+2}, \Delta t_{n+1})\mathbf{B}_{n+1} \quad (104)$$

With constant time steps,  $\mathbf{B}_{n+2} = \mathbf{B}_{n+1}$ ,  $\mathbf{D}_{n+2} = \mathbf{D}_{n+1}$  and the amplification matrices are similar. However, in variable time step, the previous relationships show that they are only equivalent.

Then, the previous propositions lead to the main result of the paper, stated in the next theorem.

**Theorem 1** *The spectral stability of the variable time step central difference is the only one leading to a zero-stability analysis. Therefore, it is the only one that provides accurate and reliable stability results. Moreover, for constant time steps, the spectral stability analysis of all the formulations lead to same conditions as zero-stability analysis.*

*Proof* Because of the loss of similarity between the amplification matrices, the only method which amplification matrix's roots are equal to the roots of the generating polynomial is the multistep one. This polynomial is used to assess the zero-stability of the scheme, hence the theorem.

Thus, to predict the behaviour of the variable time step central difference scheme, one needs to calculate the stability conditions on the multistep formulation. This further motivates the assumption of Zienkiewicz [28] who noticed, thanks to a weighted residual approach, that ③ was the most comprehensive representation of the central difference method.

Therefore, to show the impact of the formulations, two time grids are created, which are predicted stable by [27], but unstable by the zero-stability analysis. Figures 4a and 4b present, for two different time steps patterns, displacement, energy balance, and time steps within the stability areas predicted by formulations ② and ③. Figure 4a is an integration with four consecutive time steps repeated in a cycle  $\Delta t_I^a = 0.95\Delta t_{cr}^e = 6.56 \times 10^{-2}$  s,  $\Delta t_{II}^a = \frac{\sqrt{2}}{2}\Delta t_{cr}^e = 4.89 \times 10^{-2}$  s,  $\Delta t_{III}^a = 0.5\Delta t_{cr}^e = 3.45 \times 10^{-2}$  s,  $\Delta t_{IV}^a = 0.7\Delta t_{cr}^e = 4.84 \times 10^{-2}$  s, while Figure 4b has two time steps  $\Delta t_I^b = 0.8\Delta t_{cr}^e = 4.68 \times 10^{-2}$  s,  $\Delta t_{II}^b = \frac{\sqrt{2}}{2}\Delta t_{cr}^e = 4.89 \times 10^{-2}$  s. We compute the energy balance of the scheme, defined in the proposition stated in the preliminaries, for  $c = 0$ :

$$\begin{aligned} & \left[ \frac{1}{2}mv^2 + \frac{1}{2}ku^2 \right]_n^{n+2} - \left( \frac{k}{m} \right)^2 \frac{m}{4} \left( \frac{1}{2}\Delta t_{n+2}^2 u_{n+2}^2 - \frac{1}{2}\Delta t_{n+1}^2 u_n^2 \right) + \\ & - \left( \frac{k}{m} \right)^2 \frac{m}{4} (\Delta t_{n+2}^2 - \Delta t_{n+1}^2) u_{n+1}^2 = 0 \end{aligned} \quad (105)$$

This energy balance takes into account that  $ma_n = -ku_n$ . With a constant time step, the term born by  $u_{n+1}^2$  vanishes and we find again the conserved pseudo energy pointed out by Krenk [17,8]. However, non-uniform discretization of time brings another energy, carried by the  $u_{n+1}^2$  term.

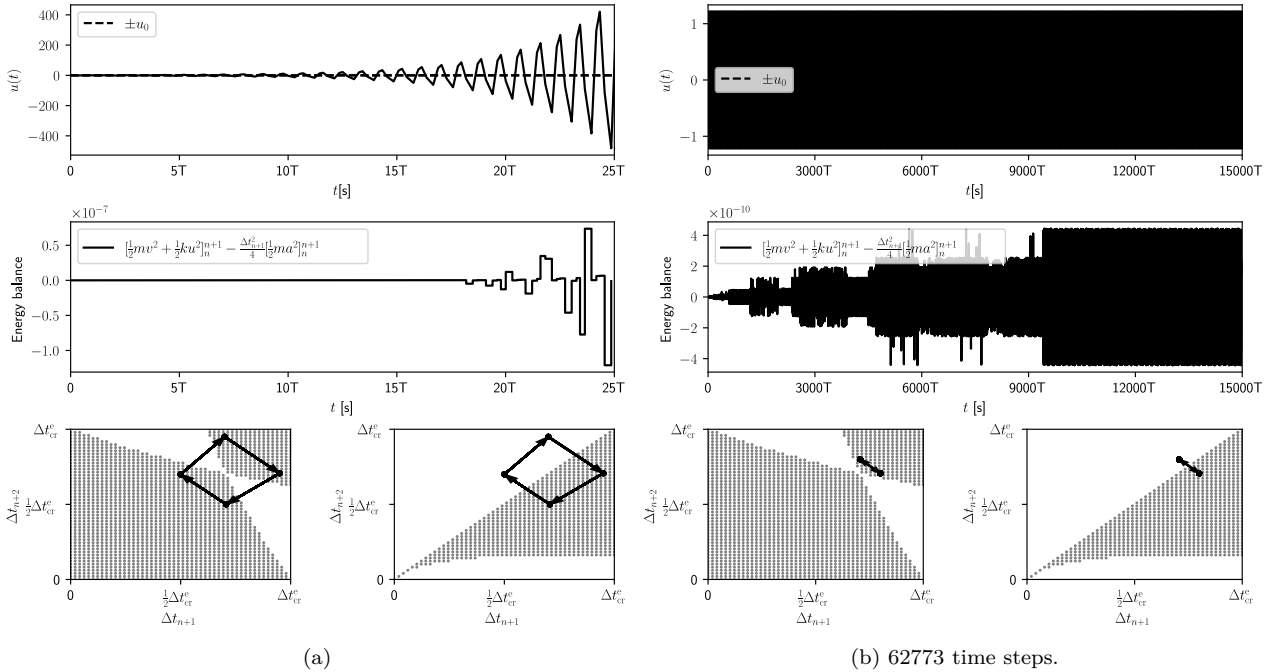


Fig. 4: Displacement, energy balance, time steps in stable zone predicted thanks to the one step and multistep formulations.

In Figure 4a, the instability appears after a few periods, and the energy balance is not conserved (we should have a balance equal to  $1 \times 10^{-14}$ , corresponding to a numerical zero). In Figure 4b, the instability appears slowly, and might not be observed in displacement, which seems to remain bounded. However, the energy balance shows a slow growth. Thus, the energy is no longer conserved within the simulation, and the scheme is unstable. These numerical experiments shows how numerical instability appear at a slow pace within a variable time step integration. Therefore, the energy balance can be useful to monitor *a posteriori* the instability, when it is not clearly displayed on common displacement, velocity fields.

This part showed that stability analysis must be performed on the linear multistep form of the method, to ensure that the zero-stability criteria is verified. Thus, the analysis pointed out, in the elastic case, the

impossibility of increasing the time step during the simulation. Finally, the energy balance is demonstrated as a useful tool to spot instability.

#### 4.2.2 The viscoelastic case

The next developments are held on the viscoelastic single degree of freedom system, where viscous damping is introduced in the single degree of freedom system as:

$$F_{n+1}^{\text{int}} = ku_{n+1} + cv_{n+1/2} \quad (106)$$

The multistep formulation of this method is then:

$$\begin{aligned} mu_{n+2} + \frac{\Delta t_{n+2} + \Delta t_{n+1}}{\Delta t_{n+1}} \left[ -m + \frac{1}{2} \Delta t_{n+2} \Delta t_{n+1} \left( k + \frac{1}{\Delta t_{n+1}} c \right) \right] u_{n+1} + \\ + \frac{\Delta t_{n+2}}{\Delta t_{n+1}} \left[ m - \frac{\Delta t_{n+2} + \Delta t_{n+1}}{2} c \right] u_n = \frac{1}{2} (\Delta t_{n+2} + \Delta t_{n+1}) \Delta t_{n+2} F_{n+1}^{\text{ext}} \end{aligned} \quad (107)$$

The amplification matrix is then:

$$\mathbf{A}(\Delta t_{n+2}, \Delta t_{n+1}) = \begin{pmatrix} A_{11} & A_{12} \\ A_{21} & A_{22} \end{pmatrix} \quad (108)$$

$$A_{11} = \frac{\Delta t_{n+2} + \Delta t_{n+1}}{\Delta t_{n+1}} \left( 1 - \frac{1}{2} \Delta t_{n+2} \Delta t_{n+1} \left( \frac{k}{m} + \frac{1}{\Delta t_{n+1}} \frac{c}{m} \right) \right) \quad (109)$$

$$A_{12} = -\frac{\Delta t_{n+2}}{\Delta t_{n+1}} \left( 1 - \frac{\Delta t_{n+2} + \Delta t_{n+1}}{2} \frac{c}{m} \right) \quad (110)$$

$$A_{21} = 1 \quad (111)$$

$$A_{22} = 0 \quad (112)$$

The invariants of the amplification matrix, are:

$$\det(\mathbf{A}) = \frac{\Delta t_{n+2}}{\Delta t_{n+1}} \left( 1 - \frac{\Delta t_{n+2} + \Delta t_{n+1}}{2} \frac{c}{m} \right) \quad (113)$$

$$\text{tr}(\mathbf{A}) = \frac{\Delta t_{n+2} + \Delta t_{n+1}}{\Delta t_{n+1}} \left( 1 - \frac{1}{2} \Delta t_{n+2} \Delta t_{n+1} \left( \frac{k}{m} + \frac{1}{\Delta t_{n+1}} \frac{c}{m} \right) \right) \quad (114)$$

As in the previous subsection, we study the stability conditions of the variable time step scheme.

**Proposition 6** *The stability of the variable time step central difference scheme for transient viscoelastic 0D problem leads to the following conditions:*

$$\Delta t_{n+2} \leq \frac{2}{\frac{c}{m} + \frac{1}{2} \frac{k}{m} \Delta t_{n+1}} \quad (115)$$

$$\begin{aligned} (\Delta t_{n+2} + \Delta t_{n+1})^2 \left( 1 - \frac{1}{2} \Delta t_{n+2} \Delta t_{n+1} \left( \frac{k}{m} + \frac{1}{\Delta t_{n+1}} \frac{c}{m} \right) \right)^2 + \\ - 4 \Delta t_{n+2} \Delta t_{n+1} \left( 1 - \frac{1}{2} (\Delta t_{n+2} + \Delta t_{n+1}) \frac{c}{m} \right) < 0 \end{aligned} \quad (116)$$

$$\forall c \neq 0,$$

$$\begin{cases} \forall \Delta t_{n+1} \in [2(3 - 2\sqrt{2}) \frac{m}{c}; 2(3 + 2\sqrt{2}) \frac{m}{c}] \\ \quad \mid \Delta t_{n+2} \in \mathbb{R}^+ \\ \forall \Delta t_{n+1} \in ]0, 2(3 - 2\sqrt{2}) \frac{m}{c}] \cup [2(3 + 2\sqrt{2}) \frac{m}{c}, +\infty[ \\ \quad \mid \Delta t_{n+2} \in ]0, l(\Delta t_{n+1})] \cup [g(\Delta t_{n+1}), +\infty[ \\ \quad \text{with } \begin{cases} l(\Delta t_{n+1}) = \frac{m}{c} - \frac{1}{2} \Delta t_{n+1} - \frac{m}{c} \sqrt{\frac{1}{4} \left( \frac{c}{m} \right)^2 \Delta t_{n+1}^2 - 3 \frac{c}{m} \Delta t_{n+1} + 1} \\ r(\Delta t_{n+1}) = \frac{m}{c} - \frac{1}{2} \Delta t_{n+1} + \frac{m}{c} \sqrt{\frac{1}{4} \left( \frac{c}{m} \right)^2 \Delta t_{n+1}^2 - 3 \frac{c}{m} \Delta t_{n+1} + 1} \end{cases} \end{cases} \quad (117)$$

*Proof* (115) is given by:

$$1 + \det(\mathbf{A}) + \text{tr}(\mathbf{A}) \geq 0 \Leftrightarrow (\Delta t_{n+2} + \Delta t_{n+1})(2 - \frac{1}{2} \Delta t_{n+2} \Delta t_{n+1} \frac{k}{m} - \Delta t_{n+2} \frac{c}{m}) \geq 0 \quad (118)$$

Since  $\Delta t_{n+1}, \Delta t_{n+2} \in \mathbb{R}^+$ , we obtain:

$$(2 - \frac{1}{2}\Delta t_{n+2}\Delta t_{n+1}\frac{k}{m} - \Delta t_{n+2}\frac{c}{m}) \geq 0 \Leftrightarrow \Delta t_{n+2} \leq \frac{2}{\frac{c}{m} + \frac{1}{2}\Delta t_{n+1}\frac{k}{m}} \quad (119)$$

(116) is given by:

$$\text{tr}^2(\mathbf{A}) - 4 \det(\mathbf{A}) < 0 \quad (120)$$

(117) is given by:

$$\begin{aligned} 1 - \det(\mathbf{A}(\Delta t_{n+2}, \Delta t_{n+1})) &\geq 0 \\ \Leftrightarrow \underbrace{\frac{1}{2}\frac{c}{m}\Delta t_{n+2}^2 + \left(-1 + \frac{1}{2}\frac{c}{m}\Delta t_{n+1}\right)\Delta t_{n+2} + \Delta t_{n+1}}_{\mathcal{P}(\Delta t_{n+2})} &\geq 0. \end{aligned} \quad (121)$$

For  $c = 0$  the condition  $1 - \det(\mathbf{A})$  leads to  $\Delta t_{n+2} \leq \Delta t_{n+1}$ . The following developments are true only for  $c \neq 0$ . The polynomial  $\mathcal{P}(\Delta t_{n+2})$  is positive for certain values of the discriminant:

$$\delta^{[\Delta t_{n+2}]}(\Delta t_{n+1}) = \frac{1}{4}\left(\frac{c}{m}\right)^2\Delta t_{n+1}^2 - 3\frac{c}{m}\Delta t_{n+1} + 1 \quad (122)$$

For:

$$\Delta t_{n+1} \in \left[2(3 - 2\sqrt{2})\frac{m}{c}; 2(3 + 2\sqrt{2})\frac{m}{c}\right] \quad (123)$$

the discriminant  $\delta^{[\Delta t_{n+2}]}(\Delta t_{n+1})$  is negative, and the polynomial  $\mathcal{P}(\Delta t_{n+2})$  remains positive for all  $\Delta t_{n+2}$ . For:

$$\Delta t_{n+1} \in \left]0, 2(3 - 2\sqrt{2})\frac{m}{c}\right] \cup \left[2(3 + 2\sqrt{2})\frac{m}{c}, +\infty\right[ \quad (124)$$

$\delta^{[\Delta t_{n+2}]}(\Delta t_{n+1})$  is positive, then the polynomial  $\mathcal{P}(\Delta t_{n+2})$  is positive for certain values of  $\Delta t_{n+2}$ , determined by its left and right roots, defined in the proposition respectively by  $l(\Delta t_{n+1})$  and  $r(\Delta t_{n+1})$ , which leads to the conditions (117) stated in the proposition.

Then, condition (115) lets us calculate the critical time step for a constant time step grid ( $\Delta t_{n+2} = \Delta t_{n+1} = \Delta t_{\text{cr}}(c)$ ):

$$\Delta t_{\text{cr}}(c) = -\frac{c}{k} + \sqrt{\left(\frac{c}{k}\right)^2 + 4\frac{m}{k}} \quad (125)$$

Furthermore, condition (117) allows for an increase in the time step during integration. In practice, only the case  $\Delta t_{n+2} \leq 2(3 - 2\sqrt{2})\frac{m}{c}$  is observed. Therefore, the upper bound of the possible increase in time step is given by  $l(\Delta t_{n+1})$ . Figure 5 shows how the stability zone evolves with the viscous damping coefficient  $c$ . The horizontal and vertical dotted lines represent the critical time step, calculated thanks to (125), for each value of  $c$ . The diagonal dotted line represents the curve on which  $\Delta t_{n+1} = \Delta t_{n+2}$ .

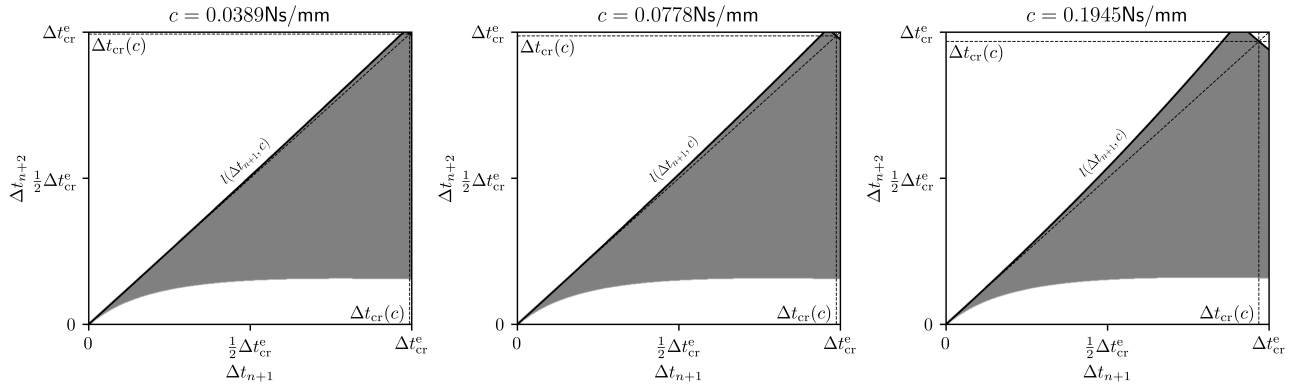


Fig. 5: Stability area for different viscous damping parameters.

Figure 6 represents displacement, energy balance (see equation (52)), and time step pattern within the stability zone for an oscillator with  $c = 1.95 \times 10^{-1} \text{ N s mm}^{-1}$ , for a time grid in which the time step increases.

The possibility of increasing the time step during the simulation is confirmed by the energy balance remaining equal to numerical zero  $1 \times 10^{-14}$ . Even if the simulation lacks accuracy, its stability is ensured by the proposed analysis.

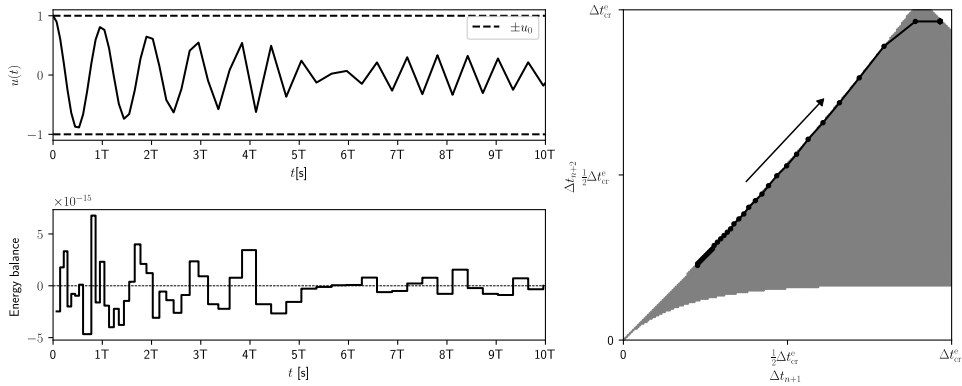


Fig. 6: Displacement, energy balance, and time step pattern within the stability zone for an oscillator with  $c = 1.95 \times 10^{-1} \text{ N s mm}^{-1}$ .

## 5 Conclusions

In this paper, we have presented for the first time the  $\alpha$  viscous stress averaging scheme for explicit transient dynamics viscoelastic continuum problems. This method has been shown to have improved stability properties for the central difference method, in particular for highly viscously damped materials.

Then, the second aim of this study was to provide a new stability analysis of variable time step central difference method. The analysis showed that the spectral stability criteria was no longer relevant for other formulation of the scheme than the multistep one. Indeed, variable time step creates a loss of spectral similarity between the different formulations existing in the literature (half step, one step, multistep). Thus, we provided analytic stability conditions for a single degree of freedom oscillator. We showed that, without viscous damping, the time step is constrained to reduce through the computation. However, with viscous damping, the time step can increase under an analytic limit that has been provided. Example of computations were presented, emphasizing the role of the energy balance to spot instability that may occur within the time integration.

## Declarations

**Conflict of interest** The authors declare that they have no conflict of interest.

**Funding** The authors have no relevant financial or non-financial interests to disclose.

**Availability of Data and Materials** Not applicable.

## References

1. Abraham, R., Marsden, J.E.: Foundations of Mechanics, 2d ed., rev., enl., and reset edn. Benjamin/Cummings Pub. Co, Reading, Mass (1978)
2. Belytschko, T., Liu, W.K., Moran, B., Elkhodary, K.I.: Nonlinear Finite Elements for Continua and Structures, second edn. Wiley, Chichester, West Sussex, United Kingdom (2014)
3. Calvo, M.P., Sanz-Serna, J.M.: The Development of Variable-Step Symplectic Integrators, with Application to the Two-Body Problem. SIAM Journal on Scientific Computing **14**(4), 936–952 (1993). DOI 10.1137/0914057
4. Casadei, F., Halleux, J.P.: Binary spatial partitioning of the central-difference time integration scheme for explicit fast transient dynamics. International Journal for Numerical Methods in Engineering **78**(12), 1436–1473 (2009). DOI 10.1002/nme.2533
5. Cirak, F., West, M.: Decomposition contact response (DCR) for explicit finite element dynamics. International Journal for Numerical Methods in Engineering **64**(8), 1078–1110 (2005). DOI 10.1002/nme.1400
6. Dahlquist, G.: Convergence and stability in the numerical integration of ordinary differential equations. Mathematica Scandinavica **4**(1), 33–53 (1956)
7. Di Stasio, J., Dureisseix, D., Gravouil, A., Georges, G., Homolle, T.: Benchmark cases for robust explicit time integrators in non-smooth transient dynamics. Advanced Modeling and Simulation in Engineering Sciences **6**(1), 2 (2019). DOI 10.1186/s40323-019-0126-y
8. Fekak, F.E., Brun, M., Gravouil, A., Depale, B.: A new heterogeneous asynchronous explicit–implicit time integrator for nonsmooth dynamics. Computational Mechanics **60**(1), 1–21 (2017). DOI 10.1007/s00466-017-1397-0
9. Gérardin, M., Rixen, D.: Mechanical Vibrations: Theory and Application to Structural Dynamics, third edn. Wiley, Chichester, West Sussex, United Kingdom (2015)
10. Hairer, E., Lubich, C., Wanner, G.: Geometric numerical integration illustrated by the Störmer–Verlet method. Acta Numerica **12**, 399–450 (2003). DOI 10.1017/S0962492902000144
11. Hairer, E., Wanner, G., Nørsett, S.P.: Solving Ordinary Differential Equations I, Springer Series in Computational Mathematics, vol. 8. Springer Berlin Heidelberg, Berlin, Heidelberg (1993). DOI 10.1007/978-3-540-78862-1
12. Hughes, T.J.R.: The Finite Element Method: Linear Static and Dynamic Finite Element Analysis. Dover Publications, Mineola, NY (2000)

13. Hwang, S., Reyes, E.I., Moon, K.s., Rumpf, R.C., Kim, N.S.: Thermo-mechanical Characterization of Metal/Polymer Composite Filaments and Printing Parameter Study for Fused Deposition Modeling in the 3D Printing Process. *Journal of Electronic Materials* **44**(3), 771–777 (2015). DOI 10.1007/s11664-014-3425-6
14. Idesman, A., Pham, D.: Finite element modeling of linear elastodynamics problems with explicit time-integration methods and linear elements with the reduced dispersion error. *Computer Methods in Applied Mechanics and Engineering* **271**, 86–108 (2014). DOI 10.1016/j.cma.2013.12.002
15. Johnsen, S.F., Taylor, Z.A., Han, L., Hu, Y., Clarkson, M.J., Hawkes, D.J., Ourselin, S.: Detection and modelling of contacts in explicit finite-element simulation of soft tissue biomechanics. *International Journal of Computer Assisted Radiology and Surgery* **10**(11), 1873–1891 (2015). DOI 10.1007/s11548-014-1142-5
16. Kane, C., Marsden, J.E., Ortiz, M., West, M.: Variational integrators and the Newmark algorithm for conservative and dissipative mechanical systems. *International Journal for Numerical Methods in Engineering* **49**(10), 1295–1325 (2000). DOI 10.1002/1097-0207(20001210)49:10<1295::AID-NME993>3.0.CO;2-W
17. Krenk, S.: Energy conservation in Newmark based time integration algorithms. *Computer Methods in Applied Mechanics and Engineering* **195**(44-47), 6110–6124 (2006). DOI 10.1016/j.cma.2005.12.001
18. Lax, P.D., Richtmyer, R.D.: Survey of the stability of linear finite difference equations. *Communications on Pure and Applied Mathematics* **9**(2), 267–293 (1956). DOI 10.1002/cpa.3160090206
19. Lew, A., Marsden, J.E., Ortiz, M., West, M.: Variational time integrators. *International Journal for Numerical Methods in Engineering* **60**(1), 153–212 (2004). DOI 10.1002/nme.958
20. Naghibi Beidokhti, H., Janssen, D., Khoshgoftar, M., Sprengers, A., Perdahcioglu, E.S., Van Den Boogaard, T., Verdonschot, N.: A comparison between dynamic implicit and explicit finite element simulations of the native knee joint. *Medical Engineering & Physics* **38**(10), 1123–1130 (2016). DOI 10.1016/j.medengphy.2016.06.001
21. Newmark, N.M.: A Method of Computation for Structural Dynamics. *Journal of the Engineering Mechanics Division* **85**(3), 67–94 (1959). DOI 10.1016/JMCEA3.0000098
22. Prevost, T.P., Balakrishnan, A., Suresh, S., Socrate, S.: Biomechanics of brain tissue. *Acta Biomaterialia* **7**(1), 83–95 (2011). DOI 10.1016/j.actbio.2010.06.035
23. Simo, J., Tarnow, N., Wong, K.: Exact energy-momentum conserving algorithms and symplectic schemes for nonlinear dynamics. *Computer Methods in Applied Mechanics and Engineering* **100**(1), 63–116 (1992). DOI 10.1016/0045-7825(92)90115-Z
24. Skeel, R.D.: Variable step size destabilizes the Störmer/leapfrog/verlet method. *BIT* **33**(1), 172–175 (1993). DOI 10.1007/BF01990352
25. Skeel, R.D.: Comments on “Numerical Instability due to Varying Time Steps in Explicit Wave Propagation and Mechanics Calculations” by Joseph P. Wright. *Journal of Computational Physics* **145**(2), 758–759 (1998). DOI 10.1006/jcph.1998.6072
26. Skeel, R.D., Gear, C.: Does variable step size ruin a symplectic integrator? *Physica D: Nonlinear Phenomena* **60**(1-4), 311–313 (1992). DOI 10.1016/0167-2789(92)90247-K
27. Wright, J.P.: Numerical Instability due to Varying Time Steps in Explicit Wave Propagation and Mechanics Calculations. *Journal of Computational Physics* **140**(2), 421–431 (1998). DOI 10.1006/jcph.1998.5902
28. Zienkiewicz, O.C.: A new look at the newmark, houbolt and other time stepping formulas. A weighted residual approach. *Earthquake Engineering & Structural Dynamics* **5**(4), 413–418 (1977). DOI 10.1002/eqe.4290050407